

TEXTURE FEATURE EXTRACTION TO IMPROVE ACCURACY OF MALIGNANT AND BENIGN CANCER DETECTION ON CT-SCAN IMAGES

Sri Widodo ^{1*}, Ibnu Rosyid ², Mohammad Faizuddin Bin MD Noor ³, Roslan Bin Ismail ⁴

Abstract: Lung cancer is a type of lung disease characterized by uncontrolled cell growth in lung tissue, whereas nodules (benign cancer) are small, round or egg-shaped lesions in the lungs. The current method used to diagnose lung cancer from CT scan images is by observing a data set of 2-D CT Scan images using the naked eye, then interpreting data one by one. This procedure is certainly not sufficient. Research conducted aims to extract texture features to improve the accuracy of malignant and benign cancers detection in CT scans. This research covers 5 (five) main points. The first is pre-processing CT-Scan images. The second is the automatic segmentation of lung area using the Active Appearance Model (AAM) method. The third is the segmentation of candidates who are considered cancer using morphological mathematics. Fourth, the process of detecting benign and malignant lung cancer is using Support Vector Machine (SVM). The fifth is the visualization of malignant and benign lung cancer using Volume Rendering. Accuracy of malignant and benign cancers detection is 79.7%.

Keywords: AAM, CT Scan, lung cancer, mathematical morphology, SVM

1. INTRODUCTION

Lung cancer is a type of lung disease characterized by uncontrolled cell growth in lung tissue (American Lung Association, 2018) (Niknam et al., 2011), whereas nodules (benign cancer) are small, round or egg-shaped lesions in the lungs. Lung nodules or benign cancers usually have a diameter of 3-4 cm (no larger than 6 cm) and are always surrounded by healthy lung tissue (Halmos et al., 2019)(Thompson et al., 2019)(Kustanto, Widodo & Tomo, 2015)(Zhou et al., 2016)(Abbas, 2017)(Tian et al., 2012)(Song et al., 2017)(Tran et al., 2019). Pulmonologists and radiologists only rely on naked-eye vision to read and diagnose both benign and malignant lung cancer on CT 2-D images. The reading process is done by putting CT and X-ray images of the print-out on the reading lamp. This technique is certainly less useful. Besides lung specialist, doctors can differ in diagnosing lung cancer, including benign or malignant, including determining the type, shape, size, and location of cancer in the lung organs (Makaju et al., 2018)(Chen et al., 2017)(Colakoglu et al., 2019). Therefore, we need an application that can detect or diagnose benign or malignant lung cancer from CT images automatically.

¹ Sri Widodo is a doctoral scholar at Health Science Faculty, Duta Bangsa University, Indonesia.

² Ibnu Rosyid is a doctoral scholar at Radiology Department, Ir. Soekarno General Hospital, Indonesia.

³ Mohammad Faizuddin Bin MD Noor is a doctoral scholar at Unkl Malaysian Institute of Information Technology, Universiti Kuala Lumpur, Kuala Lumpur.

⁴ Roslan Bin Ismail is a doctoral scholar Unkl Malaysian Institute of Information Technology, Universiti Kuala Lumpur, Kuala Lumpur.

*Correspondence Email: papa_lucky10@yahoo.com

Several studies on the detection of lung cancer using intelligent systems have been carried out (Adetiba & Olugbara, 2015)(Sasikala et al., 2018)(Mesleh, 2017)(Anuja & Smitha Vas, 2019)(Abbas, 2017)(Kadir & Gleeson, 2018)(Jakimovski & Davcev, 2019)(Pehrson et al., 2019)(Pandiangan et al., 2019)(Jeya & Deepa, 2016)(Dandil, 2018). These studies include research from Bhagyashri (Patil & Jain, 2014), namely the detection of lung cancer cells on CT-Scan using image processing methods. The segmentation method used is thresholding and floating watershed method. Meanwhile, to predict lung cancer using a binarization approach and masking process. The segmentation method with a watershed has an accuracy of 85.27%, while segmentation using Thresholding has an accuracy of 81.24%.

The second study is a study from Vijay A. Gajdhane (A.Gajdhane & L.M, 2014) is the detection of lung cancer on CT-Scan images using various image processing techniques. First, preprocessing using filter Gabor and segmentation using watershed. For Region of Interest (ROI) extraction using three features, namely, the area is the number of white pixels in the extracted plane, the perimeter is the length of the boundary of Region of Interest (ROI) extracted, and eccentricity is the shape of a round object. Classification using Support vector machines method. The third study is research from Disha Sharma (Sharma & Jindal, 2011) is the identification of lung cancer using image processing techniques. The study begins with preprocessing stages of the image, namely removal of noise (noise), and improvement of image quality using Wiener filters. Features used to identify cancers are ROI, calcification, shape, nodule size, and contrast improvement. The accuracy obtained is 80%.

The next study was research from Mokhled (Al-tarawneh et al., 2014), who researched the detection of lung cancer using image processing techniques. The study began with image processing to improve the quality of images using Gabor and Gaussian Filters. Segmentation uses Binarization and Masking Approach. Features used for the classification process are pixels percentage and mask-labeling. The accuracy obtained is 85.7%. From the description above, it can be seen that all methods used for lung segmentation and cancer and nodule candidates use conventional methods that rely solely on the contrast value of image margins. The disadvantage of this method is if the shape of cancer is significant and affects the lung border, resulting in unclear lung borders, so if the segmentation of cancer image is the main focus, it is not included in the lung image so that segmentation will fail. In addition, the features used are too few, so the classification does not get maximum results.

While the research conducted is to extract texture features to improve the accuracy of malignant and benign lung cancer detection on CT-Scan images. The study was divided into 5 (five) steps. The first was pre-processing CT-Scan images. The second is the segmentation of the lung area using the Active Appearance Model (AAM) method. The third is the segmentation of candidates suspected of cancer by using mathematical morphology. Fourth is the process of detecting malignant and benign lung cancer using Support Vector Machine (SVM). The fifth is a three-dimensional (3-D) reconstruction of malignant and benign lung cancer using the volume rendering method. This research is expected to help medical staff, especially lung specialist and radiologists, as a second opinion in diagnosing benign and malignant cancers in the lungs.

2. MATERIALS AND METHODS

Dataset used was 80 CT images of pulmonary nodules from NBIA, which included cancer images (malignant and benign lung cancer) and arteries. Testing data is the result of imaging data from Ir. Soekarno General Hospital, Central Java, Indonesia. Axial slice orientation with one patient is taken from one to three slices so that the total slices used in the experiment are 50 slices. Image Size is 505x427 pixels, and thickness is 0.5-10 mm. While the size of the training data is 60x60 pixels. Examples of CT images with axial slices and tissue localization are shown in Figure 1.

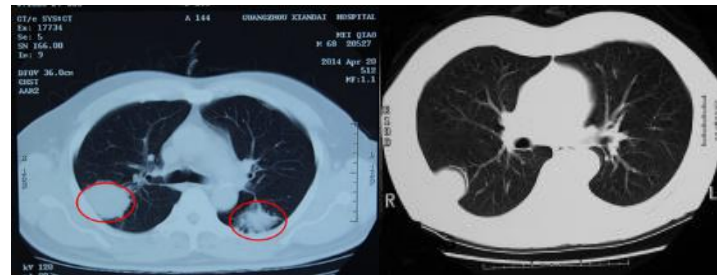


Figure 1. Left: CT Scan of Malignant Lung Cancer, Right: Benign Lung Cancer

The steps in the detection of malignant and benign lung cancer from CT-Scan images can be explained in Figure 2.

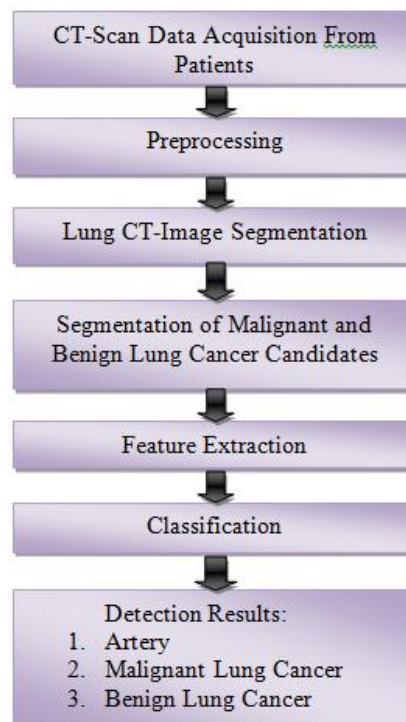


Figure 2. Steps for Detection of Malignant and Benign Lung Cancer on CT-Scan

Steps in the detection of malignant and benign lung cancer from CT-Scan images can automatically be explained as follows:

- a. The acquisition of CT scan images with axial slices was carried out in the radiology section of RSUD Ir. Soekarno Sukoharjo, Central Java. Examples of Lung Cancer CT Scan Display are shown in Figure 3.

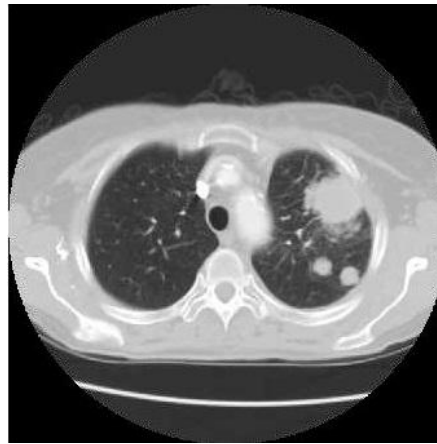


Figure 3. Example of Lung Cancer CT Scan

- b. Pre-processing:

This step consists of setting the intensity value (intensity adjustment) by means of linear mapping of the intensity value on the initial histogram to the intensity value of the new histogram and histogram equalization is a non-linear process that aims to provide the value of the image lighting in accordance with visual analysis human.

- c. Lung Segmentation:

Lung segmentation is done with the aim of separating the pulmonary organs from the surrounding tissue using the Active Appearance Model (AAM) method (Cootes et al., 2013)(Widodo et al., 2018), making it easier to detect and visualize. An example of a segmented lung image is shown in Figure 4.

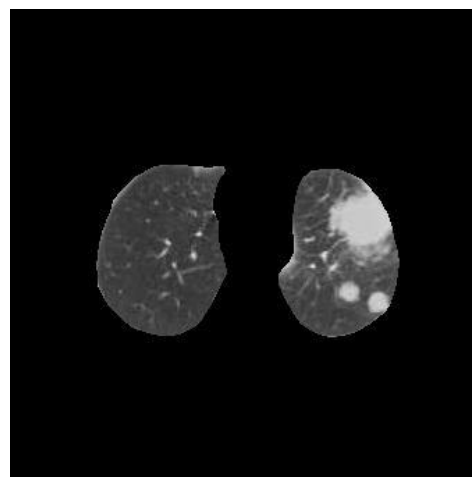


Figure 4. Final Lung Image

- d. Lung Cancer Candidates Segmentation:

Lung cancer candidate segmentation is a segmentation of lung image that is suspected to be cancer. Segmentation is carried out using mathematical morphological methods

(Jonker, 2000). The result of images that are suspected of being cancer is shown in Figure 5.

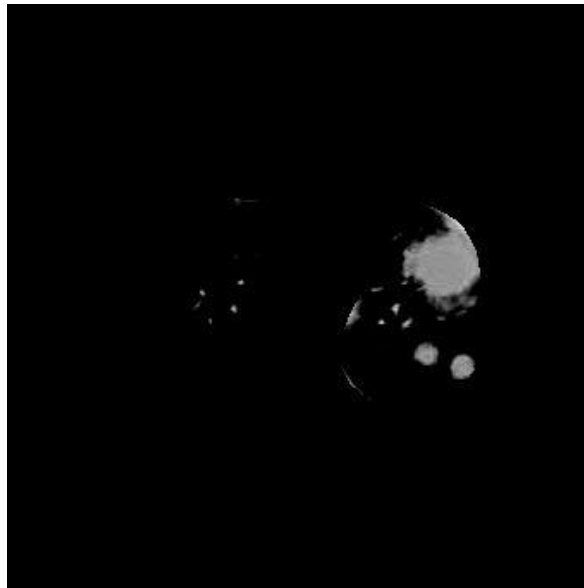


Figure 5. Image Segmentation Results Suspected as Lung Cancer

e. Feature Extraction:

Texture features (Karargyris et al., 2016)(Adams et al., 2018)(Kumar et al., 2015)(Ankita et al., 2019) used for detection of malignant and benign lung cancer from CT-scan include first-order statistical features which include: mean, standard deviation, smoothness, third moment, uniformity, entropy, and second-order statistical features (order) which includes: mean, entropy, standard deviation, variance, correlation, energy, and homogeneity. The selected features will be used for the classification process of malignant, benign and artery lung cancer

f. Lung Cancer Classification Process Not Small Cells:

The first step of the detection process is image processing to create training data. The process begins with pre-processing and segmentation using the Active Appearance Model (AAM) (Hasan Abdulameer et al., 2016)(Gao et al., 2010) for lung segmentation on CT-Scan images and mathematical morphology for segmentation suspected of being cancerous. Then normalization process such as cropping and resizing to equalize the training image dimensions of CT-Scan. The next process is feature extraction. Selected features are used for the classification process of malignant, benign of lung cancer, and artery from CT scans. Features used include first-order statistics, second-order statistics features. The classification process is then performed using Support Vector Machine (SVM) (Tian et al., 2012)(Widodo et al., 2019)(Asuntha et al., 2016). The final step is the testing process. The image used is chest CT scan data suspected of containing lung cancer that has never been trained in the training process. The result of this process is the index value of the most significant decision function, which states the class of test data. If the class produced from the testing classification process is the same as the test data class, then the recognition is declared correct. The stages of the nodule classification process can be explained in Figure 6.

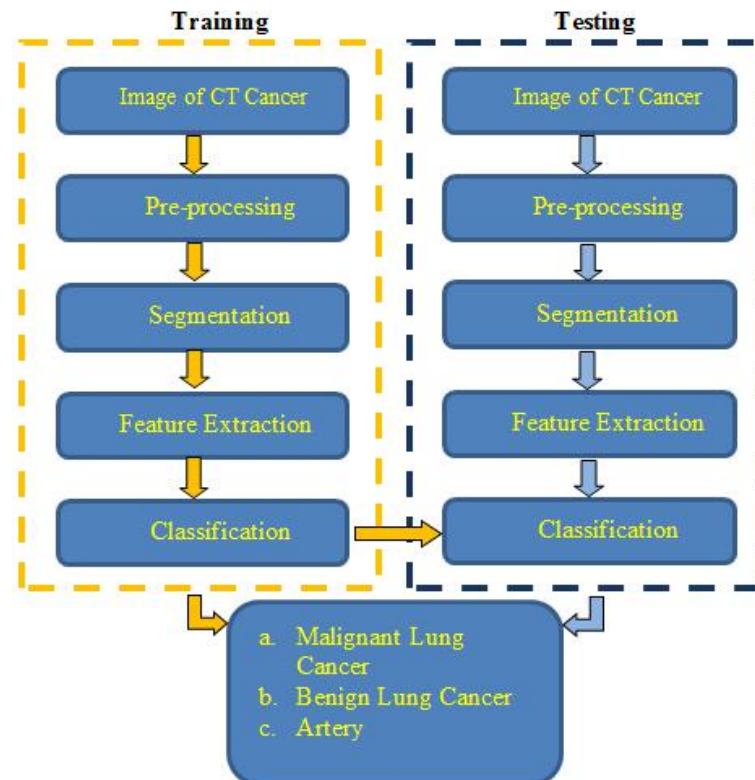


Figure 6. Steps of Classification of Malignant and Benign Lung Cancer Process

The results of classification will be compared with ground-truth so that four values will be obtained, each of which is truly positive, false negative, false positive, and true negative. True positive (TP) shows images of malignant, benign, and artery of lung cancer that are identified precisely according to their class. False-positive (FP) is an image of malignant, benign, and artery lung cancer that should be correctly identified in its class turns out to be in the classification process in identifying wrong. True negative (TN) is an image that is not a member of the class correctly identified as not a member of the class. Negative false (FN) indicates the image of a nodule that should not be a member of the class identified as a member of the class. Based on the four values, a true positive rate (TPR) value, known as sensitivity, is obtained. The sensitivity formula is as follows:

$$TPR = \frac{TP}{TP+FN} \quad (1)$$

False-positive rate (FPR) or specificity is a value that indicates the level of error in identification obtained based on the following equation:

$$FPR = \frac{FP}{FP+TN} \quad (2)$$

While the value that shows the accuracy of the identification (accuracy) is obtained from the following equation:

$$Accuracy = \frac{TP+TN}{TP+FP+TN+FN} \times 100\%$$

(3)

Detection results can be seen in Figure 7.

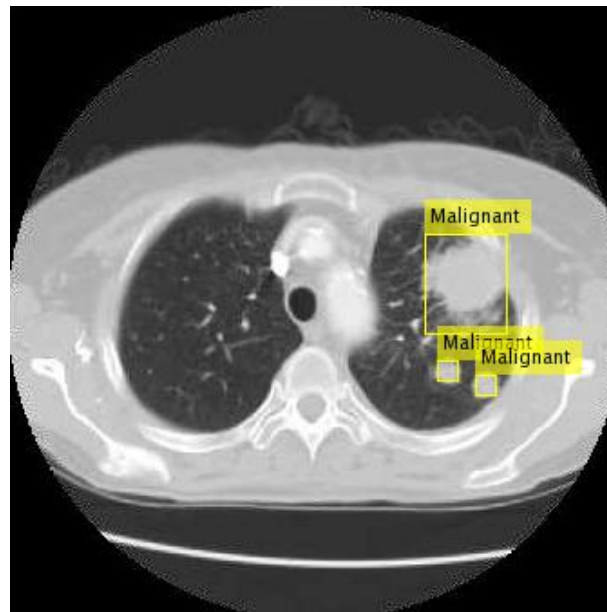


Figure 7. Lung Cancer Detection Results

g. 3-D Visualization of Lung Cancer:

The input file is a set of 2-D images contained in the same folder. A set of 2-D pulmonary CT scan images will be loaded and displayed on the screen. Reader, Mapper, and Actor are terms used that relate to the process of image visualization. Volume Rendering is the stage in which a process to reconstruct a set of 2-D lung images into 3-D (Kaufman & Mueller, 2005)(Dappa et al., 2016)(Widodo & Wijiyanto, 2014). Examples of the results of the 3-dimensional visualization of cancer in the lung organs can be seen in Figure 8.

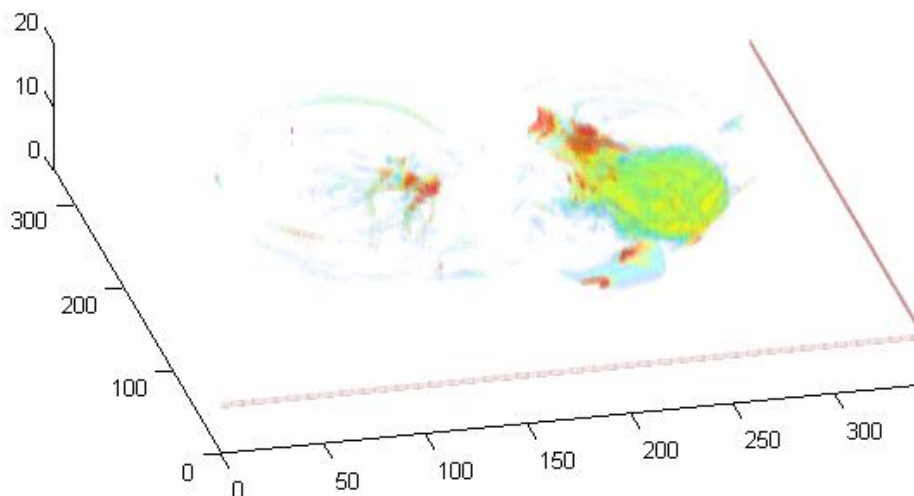


Figure 8. 3-D Visualization of Lung Cancer

3. RESULTS AND DISCUSSION

System testing is carried out after CT images of malignant, benign lung cancer and artery are segmented to separate the image of cancer from the surrounding tissue, and at the same time, to determine the Region of Interest (ROI) of the lesion object. Furthermore, the image is normalized to 60x60 pixel size with a degree of gray degree 255. The testing process is carried out using three-fold cross-validation. Data in each class is divided into three groups, with the breakdown of the first 20 data into training data, while the last 1/3 of the data (10 data) are treated as test data. Every data is being turned into test data without overlapping occurs so that all of the data has ever been testing or training data.

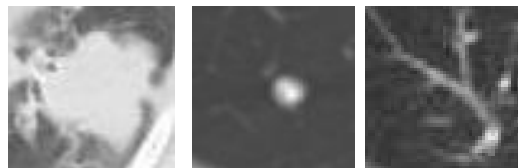


Figure 9. ROI Determination Process of Malignant, Benign, and Artery

After the ROI selection of the lesion, the object is then calculated, the value of the texture features of the object. Table 1 presents an example of the results of feature extraction in malignant cancer. Table 2 presents an example of the results of feature extraction in benign cancer. Table 3 presents an example of the results of feature extraction in the artery image.

Table 1. Feature Extraction Values in Malignant Lung Cancer

No.	Texture Features Value of Malignant Lung Cancer					
	Mean	Standard Deviation	Smoothness	Third Moment	Uniformity	Entropy
1	13.8886	37.121	0.973768	2.005589	0.61221	2.03083
2	17.3947	46.50836	0.978951	3.845632	0.670521	1.827714
3	15.6127	41.91042	0.976696	2.956574	0.630464	2.043192
4	5.90444	21.27568	0.955108	0.66567	0.639827	1.801415
5	9.09194	28.43852	0.966031	1.201045	0.642661	1.894134

Table 2. Value of Feature Extraction in Benign Lung Cancer

No.	Texture Features Value of Benign Lung Cancer					
	Mean	Standard Deviation	Smoothness	Third Moment	Uniformity	Entropy
1	1.41667	53.83169	0.981762	6.780606	0.49884	2.457804
2	1.65	16.74834	0.943657	0.799355	0.91123	0.440855
3	1.41638	14.88197	0.937036	0.589428	0.906552	0.455869
4	5.58722	29.33746	0.967037	2.235847	0.693768	1.389152
5	2.64583	20.32922	0.953116	1.122758	0.843473	0.763311

Table 3. Extraction Features Value of Artery Image

No.	Texture Features Value of Artery					
	Mean	Standard Deviation	Smoothness	Third Moment	Uniformity	Entropy
1	0.8825	22.76868	0.957928	1.116471	0.578141	1.836569
2	0.7175	7.109612	0.87669	0.097998	0.823023	0.731076

3	0.48416	15.13178	0.938011	0.483375	0.700438	1.309266
4	0.905	8.148338	0.890691	0.130276	0.810884	0.807418
5	0.46694	14.75779	0.936539	0.430292	0.686957	1.342782

The feature extraction values from the three classes are shown in Figure 10.

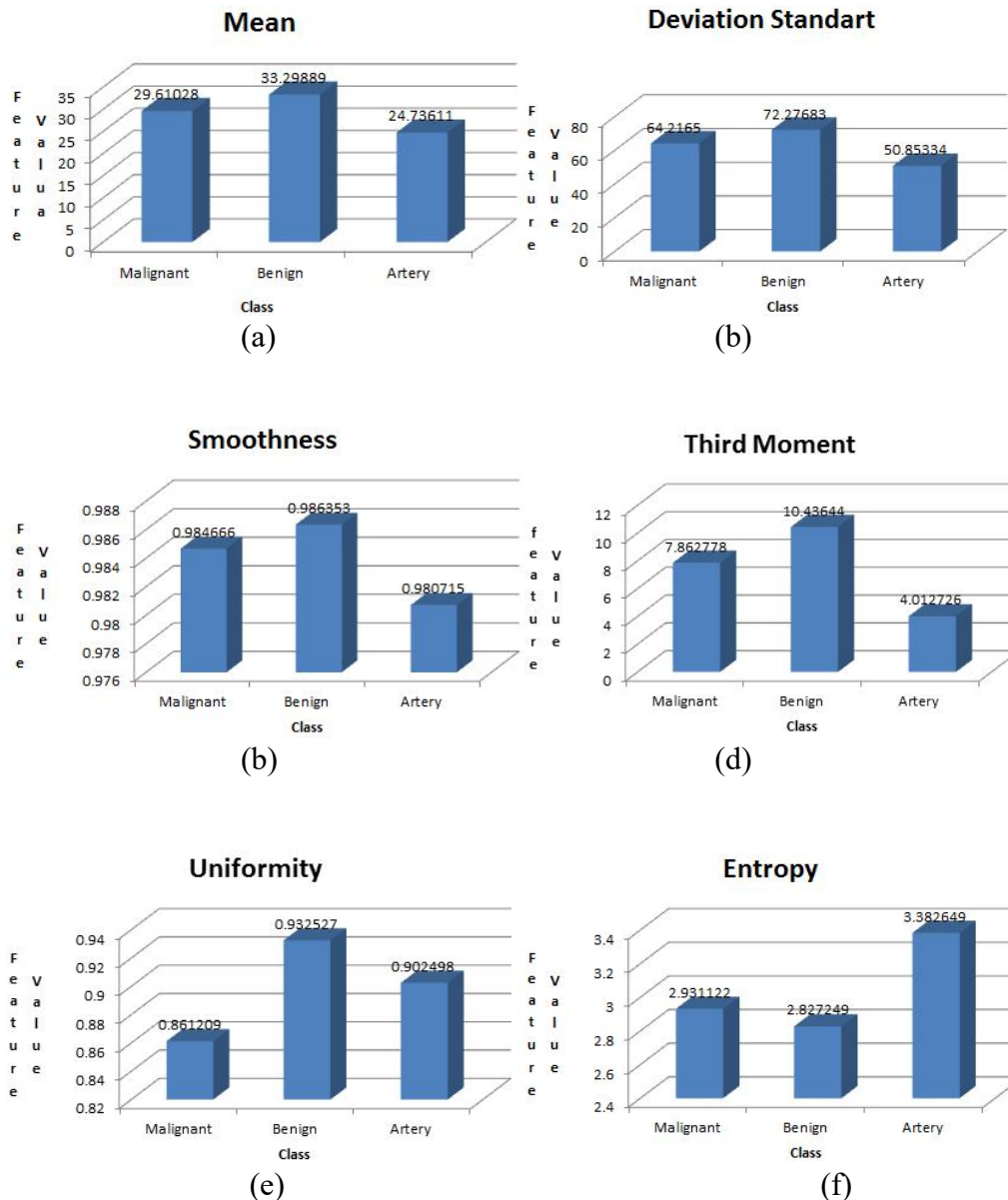


Figure 10. Graph of Range of Feature Extraction Results, (a) Mean, (b) Standard Deviation, (c) smoothness, (d) third moment, (e) uniformity, (f) entropy

Table 4. Range (Max-Min) Value of Feature Extraction Results

Fitur	Range	Malignant	Benign	Artery
Mean	Min	3.518056	0.276667	0.431389
	Max	29.61028	33.29889	24.73611
Deviation Standart	Min	19.10604	4.511542	4.481709
	Max	64.2165	72.27683	50.85334
Smoothness	Min	0.950264	0.818563	0.817575
	Max	0.984666	0.986353	0.980715

Third Moment	Min	0.561423	0.039647	0.021627
	Max	7.862778	10.43644	4.012726
Uniformity	Min	0.453147	0.438272	0.389122
	Max	0.861209	0.932527	0.902498
Entropy	Min	0.742025	0.325669	0.447531
	Max	2.931122	2.827249	3.382649

Table 4 shows features value that has been extracted from first-order statistic literature from malignant lung cancer, benign lung cancer, and artery. It can be seen that the value of the features of the three classes is overlapping. For example, the mean value of malignant lung cancer from 3.518056 to 29.61028, the value of benign lung cancer from 0.276667 to 33.29889, and arteries from 0.431389 to 24.73611. This means that using first-order statistical texture features of malignant lung cancer, benign lung cancer, and the artery is difficult to classify.

In experimental stage after classification using the Support Vector Machine (SVM) method with Gaussian and parameter values $C = 10000$, $\alpha = 1e-7$ and $\sigma = 4000$. Experiments were carried out two times, and obtained accuracy values for all rounds of testing are, on average, 79.7%.

From texture feature extraction done, it is obtained the value of the feature of three classes is overlapping. This means that using first-order statistical texture features of malignant lung cancer, benign lung cancer, and the artery is difficult to classify. So that accuracy obtained is still low. To overcome these problems, an increasing number of features and types of features needs to be done.

4. CONCLUSION

After testing, it can be concluded that by using the Support Vector Machine (SVM) classification method of 30 testing data, the performance still needs to be improved, with an average accuracy of 79.7%.

REFERENCES

- [1] A.Gajdhane, M. V., & L.M, P. D. (2014). Detection of Lung Cancer Stages on CT scan Images by Using Various Image Processing Techniques. *IOSR Journal of Computer Engineering*, 16(5), 28–35. <https://doi.org/10.9790/0661-16532835>
- [2] Abbas, Q. (2017). Nodular-Deep : Classification of Pulmonary Nodules using Deep Neural Network. *International Journal of Medical Research & Health Sciences*, 6(8), 111–118.
- [3] Adams, T., Dörpinghaus, J., Jacobs, M., & Steinhage, V. (2018). Automated lung tumor detection and diagnosis in CT Scans using texture feature analysis and SVM. *Communication Papers of the 2018 Federated Conference on Computer Science and Information Systems*, 17, 13–20. <https://doi.org/10.15439/2018f176>

- [4] Adetiba, E., & Olugbara, O. O. (2015). Lung cancer prediction using neural network ensemble with histogram of oriented gradient genomic features. *Scientific World Journal*, 2015. <https://doi.org/10.1155/2015/786013>
- [5] Al-taraweeh, M. S., Al-habashneh, S., Shaker, N., Tarawneh, W., & Tarawneh, S. (2014). *Lung Cancer Detection using*. 3(7), 1794–1798. <https://doi.org/10.15662/IJAREEIE.2019.0802011>
- [6] American Lung Association. (2018). *State of Lung Cancer*. <https://www.lung.org/our-initiatives/research/monitoring-trends-in-lung-disease/state-of-lung-cancer/>
- [7] Ankita, R., Kumari, C. U., Mehdi, M. J., Tejashwini, N., & Pavani, T. (2019). Lung cancer image-feature extraction and classification using GLCM and SVM classifier. *International Journal of Innovative Technology and Exploring Engineering*, 8(11), 2211–2215. <https://doi.org/10.35940/ijitee.K2044.0981119>
- [8] Anuja, J., & Smitha Vas, P. (2019). Deep lung cancer prediction and segmentation on CT scan. *International Journal of Engineering and Advanced Technology*, 8(5), 2308–2313.
- [9] Asuntha, A., Brindha, A., Indirani, S., & Srinivasan, A. (2016). Lung cancer detection using SVM algorithm and optimization techniques. *Journal of Chemical and Pharmaceutical Sciences*, 9(4), 3198–3203.
- [10] Chen, F., Chen, P., Muhammed, H. H., & Zhang, J. (2017). Intravoxel Incoherent Motion Diffusion for Identification of Breast Malignant and Benign Tumors Using Chemometrics. *BioMed Research International*, 2017. <https://doi.org/10.1155/2017/3845409>
- [11] Colakoglu, B., Alis, D., & Yergin, M. (2019). Diagnostic Value of Machine Learning-Based Quantitative Texture Analysis in Differentiating Benign and Malignant Thyroid Nodules. *Journal of Oncology*, 2019. <https://doi.org/10.1155/2019/6328329>
- [12] Cootes, T. F., Edwards, G., & Taylor, C. J. (2013). *Comparing Active Shape Models with Active Appearance Models*. January 1999, 18.1-18.10. <https://doi.org/10.5244/c.13.18>
- [13] Dandil, E. (2018). A computer-aided pipeline for automatic lung cancer classification on computed tomography scans. *Journal of Healthcare Engineering*, 2018. <https://doi.org/10.1155/2018/9409267>
- [14] Dappa, E., Higashigaito, K., Fornaro, J., Leschka, S., Wildermuth, S., & Alkadhi, H. (2016). Cinematic rendering – an alternative to volume rendering for 3D computed

tomography imaging. *Insights into Imaging*, 7(6), 849–856.
<https://doi.org/10.1007/s13244-016-0518-1>

- [15] Gao, X., Su, Y., Li, X., & Tao, D. (2010). A review of active appearance models. *IEEE Transactions on Systems, Man and Cybernetics Part C: Applications and Reviews*, 40(2), 145–158. <https://doi.org/10.1109/TSMCC.2009.2035631>
- [16] Halmos, B., Tan, E. H., Soo, R. A., Cadranel, J., Lee, M. K., Foucher, P., Hsia, T. C., Hochmair, M., Griesinger, F., Hida, T., Kim, E., Melosky, B., Märten, A., & Carcereny, E. (2019). Impact of afatinib dose modification on safety and effectiveness in patients with EGFR mutation-positive advanced NSCLC: Results from a global real-world study (RealGiDo). *Lung Cancer*, 127(September 2018), 103–111. <https://doi.org/10.1016/j.lungcan.2018.10.028>
- [17] Hasan Abdulameer, M., A. Mohammed, D., Farhan Rashag, H., & D. Rjeib, H. (2016). A Review Article for Active Appearance Model Fitting Based on Optimization Methods. *Research Journal of Applied Sciences, Engineering and Technology*, 12(10), 1057–1063. <https://doi.org/10.19026/rjaset.12.2825>
- [18] Jakimovski, G., & Davcev, D. (2019). Using double convolution Neural Network for lung cancer stage detection. *Applied Sciences (Switzerland)*, 9(3). <https://doi.org/10.3390/app9030427>
- [19] Jeya, I. J. S., & Deepa, S. N. (2016). Lung cancer classification employing proposed real coded genetic algorithm based radial basis function neural network classifier. *Computational and Mathematical Methods in Medicine*, 2016. <https://doi.org/10.1155/2016/7493535>
- [20] Jonker, P. P. (2000). Morphological operations on 3D and 4D images: From shape primitive detection to skeletonization. *Lecture Notes in Computer Science (Including Subseries Lecture Notes in Artificial Intelligence and Lecture Notes in Bioinformatics)*, 1953 LNCS(March 2001), 371–391. https://doi.org/10.1007/3-540-44438-6_31
- [21] Kadir, T., & Gleeson, F. (2018). Lung cancer prediction using machine learning and advanced imaging techniques. *Translational Lung Cancer Research*, 7(3), 304–312. <https://doi.org/10.21037/tlcr.2018.05.15>
- [22] Karargyris, A., Siegelman, J., Tzortzis, D., Jaeger, S., Candemir, S., Xue, Z., Santosh, K. C., Vajda, S., Antani, S., Folio, L., & Thoma, G. R. (2016). Combination of texture and shape features to detect pulmonary abnormalities in digital chest X-rays. *International Journal of Computer Assisted Radiology and Surgery*, 11(1), 99–106. <https://doi.org/10.1007/s11548-015-1242-x>

- [23] Kaufman, A., & Mueller, K. (2005). Overview of volume rendering. *Visualization Handbook, December*, 127–174. <https://doi.org/10.1016/B978-012387582-2/50009-5>
- [24] Kumar, R., Srivastava, R., & Srivastava, S. (2015). Detection and Classification of Cancer from Microscopic Biopsy Images Using Clinically Significant and Biologically Interpretable Features. *Journal of Medical Engineering*, 2015, 1–14. <https://doi.org/10.1155/2015/457906>
- [25] Kustanto, Widodo, S., & Tomo. (2015). Software Development To Detect Lung Nodules in Computed Tomography Scan Image Using Support Vector Machine. *International Research Journal of Engineering and Technology (IRJET)*, 02(06), 354–360. www.irjet.net
- [26] Makaju, S., Prasad, P. W. C., Alsadoon, A., Singh, A. K., & Elchouemi, A. (2018). Lung Cancer Detection using CT Scan Images. *Procedia Computer Science*, 125(2009), 107–114. <https://doi.org/10.1016/j.procs.2017.12.016>
- [27] Mesleh, A. M. (2017). Lung cancer detection using multi-layer neural networks with independent component analysis: A comparative study of training algorithms. *Jordan Journal of Biological Sciences*, 10(4), 239–249.
- [28] iknam, F., Chen, J., Napaki, S., & Aghmesheh, M. (2011). Approach to multiple pulmonary nodules: A case report and review of literature. *TheScientificWorldJournal*, 11, 760–765. <https://doi.org/10.1100/tsw.2011.74>
- [29] Pandiangan, T., Bali, I., & Silalahi, A. R. J. (2019). Early lung cancer detection using artificial neural network. *Atom Indonesia*, 45(1), 9–15. <https://doi.org/10.17146/aij.2019.860>
- [30] Patil, B. G., & Jain, S. N. (2014). Cancer Cells Detection Using Digital Image Processing Methods. *International Journal of Latest Trends in Engineering and Technology*, 3(4), 45–49.
- [31] Pehrson, L. M., Nielsen, M. B., & Lauridsen, C. A. (2019). Automatic pulmonary nodule detection applying deep learning or machine learning algorithms to the LIDC-IDRI database: A systematic review. *Diagnostics*, 9(1). <https://doi.org/10.3390/diagnostics9010029>
- [32] Sasikala, S., Bharathi, M., & Sowmiya, B. R. (2018). Lung cancer detection and classification using deep CNN. *International Journal of Innovative Technology and Exploring Engineering*, 8(2S), 259–262.

- [33] Sharma, D., & Jindal, G. (2011). Identifying Lung Cancer Using Image Processing Techniques. *International Conference on Computational Technique and Artificial Intelligence*, 115–120.
- [34] Song, Q. Z., Zhao, L., Luo, X. K., & Dou, X. C. (2017). Using Deep Learning for Classification of Lung Nodules on Computed Tomography Images. *Journal of Healthcare Engineering*, 2017. <https://doi.org/10.1155/2017/8314740>
- [35] Thompson, J. C., Fan, R., Black, T., Yu, G. H., Savitch, S. L., Chien, A., Yee, S. S., Sen, M., Hwang, W. T., Katz, S. I., Feldman, M., Vachani, A., & Carpenter, E. L. (2019). Measurement and immunophenotyping of pleural fluid EpCAM-positive cells and clusters for the management of non-small cell lung cancer patients. *Lung Cancer*, 127(August 2018), 25–33. <https://doi.org/10.1016/j.lungcan.2018.11.020>
- [36] Tian, Y., Shi, Y., & Liu, X. (2012). Recent advances on support vector machines research. *Technological and Economic Development of Economy*, 18(1), 5–33. <https://doi.org/10.3846/20294913.2012.661205>
- [37] Tran, G. S., Nghiem, T. P., Nguyen, V. T., Luong, C. M., Burie, J. C., & Levin-Schwartz, Y. (2019). Improving Accuracy of Lung Nodule Classification Using Deep Learning with Focal Loss. *Journal of Healthcare Engineering*, 2019. <https://doi.org/10.1155/2019/5156416>
- [38] Widodo, S., Rohmah, R. N., & Handaga, B. (2018). Classification of lung nodules and arteries in computed tomography scan image using principle component analysis. *Proceedings - 2017 2nd International Conferences on Information Technology, Information Systems and Electrical Engineering, ICITISEE 2017, 2018-Janua*, 153–158. <https://doi.org/10.1109/ICITISEE.2017.8285485>
- [39] Widodo, S., Rohmah, R. N., Handaga, B., & Arini, L. D. D. (2019). Lung diseases detection caused by smoking using support vector machine. *Telkomnika (Telecommunication Computing Electronics and Control)*, 17(3), 1256–1266. <https://doi.org/10.12928/TELKOMNIKA.V17I3.9799>
- [40] Widodo, S., & Wijiyanto. (2014). Software development for three dimensional visualization of lung on computed tomography scans using active shape model and volume rendering. *Journal of Theoretical and Applied Information Technology*, 65(1), 154–160.
- [41] Zhou, T., Lu, H., Zhang, J., & Shi, H. (2016). Pulmonary nodule detection model based on SVM and CT image feature-level fusion with rough sets. *BioMed Research International*, 2016. <https://doi.org/10.1155/2016/8052436>